

Parametrized Model Order Reduction for Component-to-System Synthesis

or

PDE Apps for Acoustic Ducts
(and Elastic Shafts, Historic Structures, Thermal Fins, . . .)

Anthony T Patera
Massachusetts Institute of Technology

CEMRACS 2016

Luminy, France
July 29, 2016

The Akselos, S.A.,¹ Team: computational methods, software, and pedagogy.

Ho Chi Minh City: *Phuong Huynh*, *Loi Nguyen*,
Tuyen Hoang, Thuc Nguyen

Boston: *David Knezevic*, Brian Sabbey

Lausanne: Thomas Leurent, Sylvain Vallaghé

¹Akselos, S.A., licenses technology developed in the MIT research group of ATP. ATP has *no financial interest* in Akselos, S.A.

P Dahl U Washington

SC Joyce SUTD

JD Penn MIT

K Smetana (U Münster, MIT)

T Taddei MIT

D Vignon MIT

M Yano U Toronto

²None of the academic collaborators has any financial interest in Akselos, S.A.

US AFOSR/Office of Secretary of Defense (— 9/2015)

US Office of Naval Research (— 5/2016)

Singapore University of Technology and Design

Ford Professorship, MIT

Parametrized Partial Differential Equations (PDEs)

- General Setting
- PDE Apps

Parametrized Partial Differential Equations (PDEs)

- General Setting
- PDE Apps

Acoustics Preliminaries

Time domain and frequency domain: Laplace transform

$$\text{pressure}(\mathbf{x}, t) = \Re\{u(\mathbf{x}, f) \exp(2\pi i f t)\}.$$

Frequency-domain pressure satisfies Helmholtz equation:

$$-\underbrace{(1 + i\epsilon k)}_{\kappa} \nabla^2 u - \underbrace{\frac{(2\pi f)^2}{c_{\text{sound}}^2}}_{k^2} u = 0 ,$$

for ϵ a dissipation coefficient and c_{sound} speed of sound.

Particle velocity is related to pressure by

$$\text{velocity}(\mathbf{x}, f) = \frac{i}{2\pi f \rho} \nabla u(\mathbf{x}, f) ,$$

for ρ the (uniform) density.

Examples of Parametrized PDEs

Heat Transfer (Conduction):

$$-\nabla(\sigma \nabla u) = q \text{ in } \Omega_\lambda, \quad s \equiv \bar{u}_{\text{root}}.$$

Linear Elasticity:

$$-\frac{\partial}{\partial x_j} E_{ijklm} \frac{\partial u_\ell}{\partial x_m} = F_i \text{ in } \Omega_\lambda, \quad s \equiv \text{SCF}.$$

Helmholtz Acoustics:

$$-(1 + i\epsilon k) \nabla^2 u - k^2 u = F \text{ in } \Omega_\lambda, \quad s \equiv Z^{\text{inlet}}.$$

INPUT PARAMETER $\mu \equiv (k, \lambda) \in \mathbb{R}^P$

\rightarrow FIELD $u_\mu(x)$ and OUTPUT (QoI) s_μ

Given $\mu \in \mathcal{P}$ (compact) $\subset \mathbb{R}^P$, find

field $u_\mu \in X(\Omega_\mu)$ (say) scalar, real

$$A_\mu u_\mu = F_\mu \text{ in } \Omega_\mu, \text{ or}$$

$$\langle A_\mu u_\mu, v \rangle = \langle F_\mu, v \rangle, \forall v \in X, \text{ or}$$

$$a_\mu(u_\mu, v) = F_\mu(v), \forall v \in X,$$

output(s) $s_\mu \in \mathbb{R}$

$$s_\mu = \langle L_\mu, u_\mu \rangle, \text{ or } s_\mu = \ell_\mu(u_\mu),$$

where $\Omega_\mu \subset \mathbb{R}^3$, $X = H_{(0)}^1(\Omega_\mu)$, and $F_\mu, L_\mu \in X'$.

Note boundary conditions are included in a_μ and F_μ .

Model and Family

A *Model* is a particular problem definition:

parametrization: $\mu \in \mathcal{P} \subset \mathbb{R}^P$;

spatial domain: $x \in \Omega_\mu \subset \mathbb{R}^3$;

physical discipline: a_μ, F_μ ;

engineering outputs (QoI): ℓ_μ .

A Model maps parameter $\mu \in \mathcal{P}$ to
field $u_\mu(x)$ and output(s) s_μ .

A *Family* is a set of Models which share
a physical discipline and engineering context.

Acoustic Ducts, Elastic Shafts, Historic Structures, . . .

Parametrized Partial Differential Equations (PDEs)

- General Setting
- PDE Apps

A PDE App is

software associated to a Model

which maps any $\mu \in \mathcal{P}$ to an

$$\text{approximate} \begin{cases} \text{field } \tilde{u}_\mu(x) & \approx u_\mu(x) \\ \text{output } \tilde{s}_\mu = \ell_\mu(\tilde{u}_\mu) & \approx s_\mu \end{cases}$$

subject to performance requirements:

response time and accuracy.

A *deployed* PDE App should satisfy:

- 5-second problem set-up time; "app-ification"
- 5-second problem solution time, field and outputs;
- 5% solution error, specified metrics;
- 5-second field visualization time.

The choice of 5 seconds is informed by
the human attention span: *interaction*.

Offline I: Very Slow — Days

Given Family, form associated Online Dataset \mathbb{D} .

Offline II: Slow — Hours

Given Model \in Family, script PDE App.

Online: Fast — Seconds

Given PDE App, evaluate $\mu \in \mathcal{P} \xrightarrow{\mathbb{D}} \tilde{u}_\mu(x), \tilde{s}_\mu$.

The PDE App Offline-Online approach
is computationally competitive in
the **many-query** context — Offline amortized, and
the **interactive** context — Offline "irrelevant."

Computational Methodology

- Perspective
- Components and System Synthesis
- Finite Element (FE) Approximation
- Static Condensation Reformulation of FE
- Model Order Reduction
- Remarks
- Computational Procedure: PDE App Workflow

Computational Methodology

- Perspective
- Components and System Synthesis
- Finite Element (FE) Approximation
- Static Condensation Reformulation of FE
- Model Order Reduction
- Remarks
- Computational Procedure: PDE App Workflow

Genetic Lines (Extensive References at Conclusion)

Component Mode Synthesis, 1960s	PR
Hurty, Craig-Bampton, Bourquin, Hetmaniuk, . . .	
Static Condensation 1970s	SC
Reduced Basis Methods, 1980s	RB
Almroth, Noor, Porsching, Gunzburger, . . .	
Post-Modern Reduced Basis Methods, 2000s	
MoRePaS I-III: <i>a priori/posteriori</i> error estimation, Weak Greedy sampling, (approximate) affine expansions, strict Offline-Online decomposition, . . .	
Reduced Basis Element Method, 2000s	E
Maday-Rønquist	

Computational Methodology

- Perspective
- **Components and System Synthesis**
- Finite Element (FE) Approximation
- Static Condensation Reformulation of FE
- Model Order Reduction
- Remarks
- Computational Procedure: PDE App Workflow

Parametrized Archetype Component

Bend

port 1

`Bend.ref_spatial_domain, Bend.ref_FE_mesh`

`Bend.port.type.ref_FE_submesh`

`Bend.parameter.angle, .rad_ratio, .k`

`Bend.parameter_domain.angle, .rad_ratio, .k`

`Bend.mapping.functions, .coefficients`

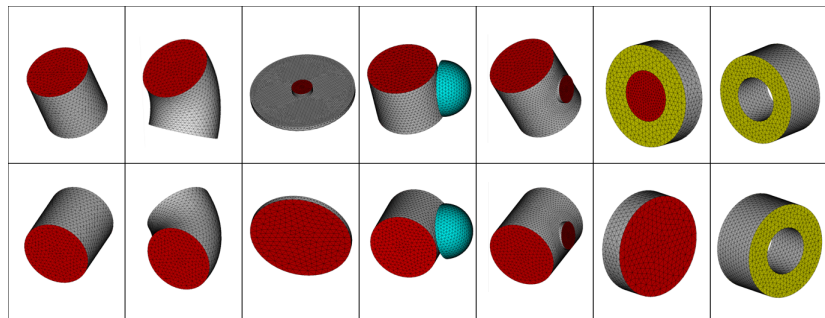
`Bend.PDE.forms.a = $\int (1 + i\epsilon k) \nabla w \cdot \nabla v - k^2 w v$`

`Bend.PDE.forms.F = 0`

spatial domain

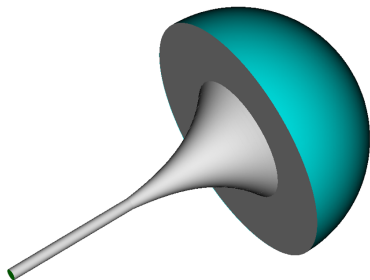
FE mesh

Acoustic Ducts
(selected archetype components)



Admissible connections:

ports of common color \leftrightarrow common port type.

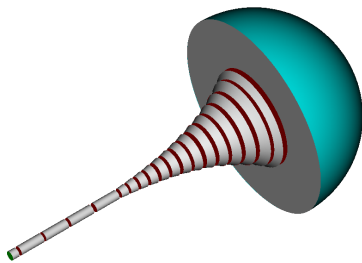
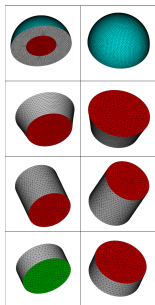


Model_Exponential_Horn (Flanged)

$$\mu \equiv (L/a_0, m^{\text{horn}}, a_{\text{mouth}}/a_0, ka_0)$$

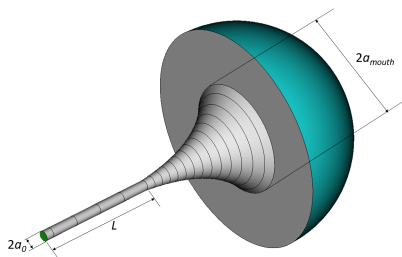
$$\in \mathcal{P} \equiv [2, 20] \times [0.0334, 0.1666] \times [4, 12] \times [0, 1]$$

System Synthesis: Instantiation and Connection



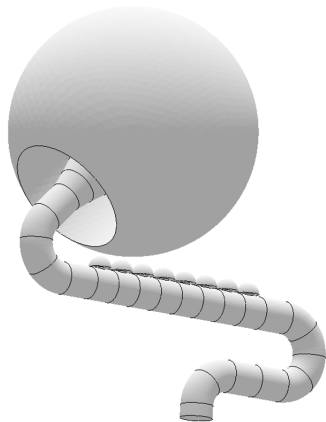
Instantiation

$$\mu_{\text{model}} \in \mathcal{P} \rightarrow \{\nu_{\text{local}} \in \mathcal{V}\}_{\text{instantiated components}}$$



Connection

$$\text{local port pairs} \rightarrow \text{global ports } \Gamma \in G$$



Model_Nguyenophone

$\mu \equiv (\text{Hole_Location}, \text{Hole_Open}, k)$

$\in \mathcal{P} \equiv \text{Wedge} \subset \mathbb{R}^8 \times \{0, 1\}^8 \times [0, 2]$

Computational Methodology

- Perspective
- Components and System Synthesis
- **Finite Element (FE) Approximation**
- Static Condensation Reformulation of FE
- Model Order Reduction
- Remarks
- Computational Procedure: PDE App Workflow

Geometry Mappings

An archetype component is characterized by

spatial domain $D_\nu =$

\mathcal{T}_ν (reference spatial domain $D_{\bar{\nu}}$)

and

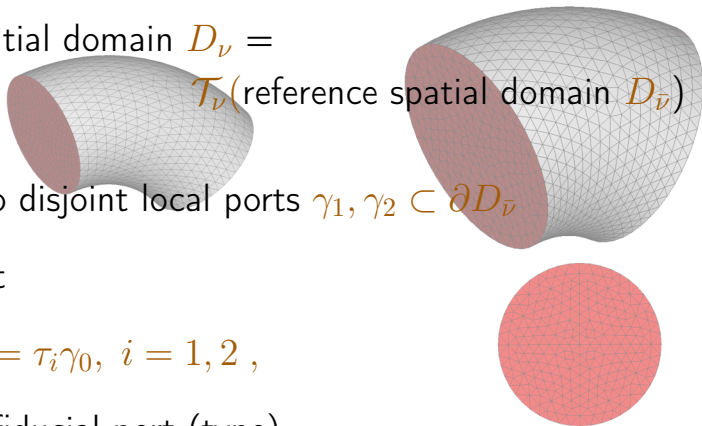
two disjoint local ports $\gamma_1, \gamma_2 \subset \partial D_\nu$

such that

$$\gamma_i = \tau_i \gamma_0, \quad i = 1, 2,$$

for γ_0 a fiducial port (type).

We may easily consider more than two local ports.



FE Approximation Spaces

Associate to

each archetype component

a reference FE mesh,

$$X^h(D_{\bar{v}}) \equiv \{v|_{T^h} \in \mathbb{P}_p(T^h), \forall T^h \in \mathbb{T}^h\}$$

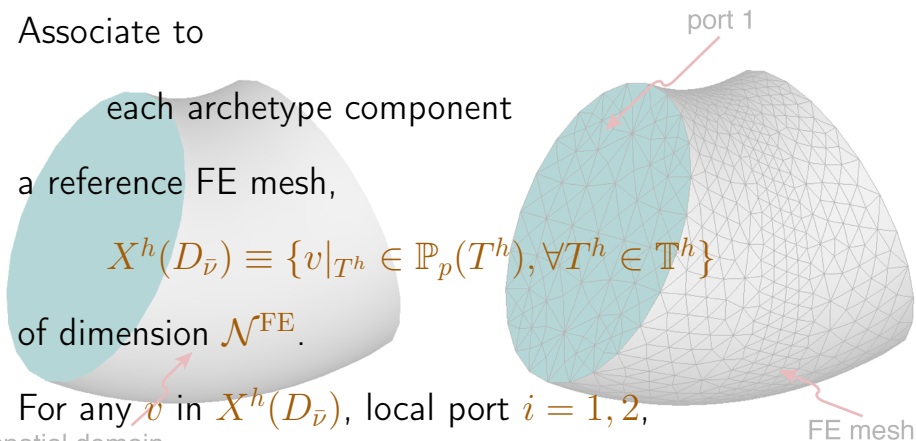
of dimension \mathcal{N}^{FE} .

For any v in $X^h(D_{\bar{v}})$, local port $i = 1, 2$,

spatial domain

$$v|_{\gamma_i} \in \left\{ \underbrace{\chi_j^{h \text{ fid}}}_{\text{fiduical port modes}} \circ \tau_i^{-1}, 1 \leq j \leq J^{\text{FE}} \right\};$$

implicit conforming condition on ports of common type.



Finite Element (FE) Approximation of Model

For given $\mu \in \mathcal{P}$, define

$$\nu = \nu(\mu)$$

$$X^h(\Omega_\mu) \equiv$$

$$\bigoplus_{\text{instantiated components}} \{v|_{D_{\bar{\nu}}} \circ \mathcal{T}_\nu^{-1} \mid v \in X^h(D_{\bar{\nu}})\} \cap X$$

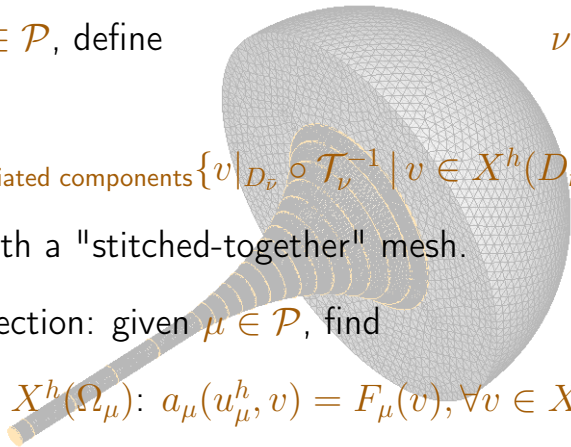
associated with a "stitched-together" mesh.

Galerkin projection: given $\mu \in \mathcal{P}$, find

$$\text{field } u_\mu^h \in X^h(\Omega_\mu): a_\mu(u_\mu^h, v) = F_\mu(v), \forall v \in X^h(\Omega_\mu),$$

and subsequently

$$\text{output } s_\mu^h = \ell_\mu(u_\mu^h).$$



Computational Methodology

- Perspective
- Components and System Synthesis
- Finite Element (FE) Approximation
- **Static Condensation Reformulation of FE**
- Model Order Reduction
- Remarks
- Computational Procedure: PDE App Workflow

Static Condensation (SC): Component Level ...

In *given instantiated component*,

$$\nu = \nu(\mu)$$

for local port $i = 1, 2$

for port mode $j = 1, \dots, J^{\text{FE}}$:

$\psi_{i,j}^h = \mathcal{L}_i(\chi_j^h \circ \tau_i^{-1})$ is lifting to

reference domain of port mode j on port i , and

$\varphi_{i,j;\nu}^h = \psi_{i,j}^h + \eta_{i,j;\nu}^h \in X_{[\gamma_1, \gamma_2; 0]}^h(D_{\bar{\nu}})$ satisfies

$a_{\nu}^{D_{\bar{\nu}}}(\varphi_{i,j;\nu}^h, v) = 0, \forall v \in X_{[\gamma_1, \gamma_2; 0]}^h(D_{\bar{\nu}})$, subject to

$$\varphi_{i,j;\nu}^h|_{\gamma_{i'}} = \chi_j^h \delta_{ii'}, \quad \mathcal{N}^{\text{FE}} \times \mathcal{N}^{\text{FE}}$$

where for simplicity all sources reside on ports.

Details

Express $\eta_{i,j;\nu}^h$ as $1 \leq j \leq J^{\text{FE}}, 1 \leq i \leq 2$

$$\eta_{i,j;\nu}^h(\bar{x}) = \sum_{k=1}^{\mathcal{N}^{\text{FE}}} \alpha_{i,j,k;\nu}^h \xi_k^h(\bar{x}) \text{ for } \bar{x} \in D_{\bar{\nu}} ;$$

then $\alpha_{i,j,k;\nu}^h$ satisfy $\mathbb{G}_{\nu} \equiv \mathbb{J}_{\nu}^{-1} \mathbb{J}_{\nu}^{-\text{T}}$

$$\begin{aligned} & \sum_{k=1}^{\mathcal{N}^{\text{FE}}} \left(\int_{D_{\bar{\nu}}} (\kappa(\nabla \xi_{k'}^{h*})^{\text{T}} \mathbb{G}_{\nu} \nabla \xi_k^h - k^2 \xi_{k'}^{h*} \xi_k^h) |\mathbb{J}_{\nu}| d\bar{x} \right) \alpha_{i,j,k;\nu}^h \\ &= - \int_{D_{\bar{\nu}}} (\kappa(\nabla \xi_{k'}^{h*})^{\text{T}} \mathbb{G}_{\nu} \nabla \psi_{i,j}^h - k^2 \xi_{k'}^{h*} \psi_{i,j}^h) |\mathbb{J}_{\nu}| d\bar{x} \end{aligned}$$

for $1 \leq k' \leq \mathcal{N}^{\text{FE}}$.

...SC: Component Level

In *given instantiated component*, (local) LINEARITY

$$u_{\mu}^h|_{D_{\nu}(\mu)} = \sum_{i=1}^2 \sum_{j=1}^{J^{\text{FE}}} u_{i,j;\nu}^h (\varphi_{i,j;\nu}^h \circ \mathcal{T}_{\nu}^{-1})$$

for appropriate coefficients $u_{i,j;\nu}^h$, $1 \leq j \leq J^{\text{FE}}$, $i = 1, 2$.

Form $2J^{\text{FE}} \times 2J^{\text{FE}}$ stiffness matrix $A_{[i,j],[k,\ell];\nu}^h$ Galerkin:

normal velocity moment on local port i flux
with respect to test port mode j

expressed in terms of

pressure coefficient on local port k
associated with trial port mode ℓ .

We may write stiffness matrix as

$$A_{[i,j],[k,l];\nu}^h \equiv \int_{D_{\bar{\nu}}} \left(\kappa(\nabla \psi_{i,j}^{h*})^T \mathbb{G}_{\nu} \nabla (\psi_{i,j}^h + \eta_{k,\ell;\nu}^h) - k^2(\psi_{i,j}^{h*})(\psi_{i,j}^h + \eta_{k,\ell;\nu}^h) \right) |\mathbb{J}_{\nu}| d\bar{x} ,$$

for $1 \leq i, k \leq 2, 1 \leq j, \ell \leq J^{\text{FE}}$.

SC: System Level

Require on global ports $\Gamma \in G$

continuity of pressure, and

weak continuity of normal velocity

implemented as direct stiffness assembly:

$$\{A_{\nu(\mu)}^h\}_{\text{instantiated components}} \rightarrow \mathcal{A}_{\mu}^h \quad ; \quad \mathcal{F}_{\mu}^h$$

here \mathcal{A}_{μ}^h is $|G|J^{\text{FE}} \times |G|J^{\text{FE}}$ block-sparse Schur complement.

Issues: J^{FE} will be large, and

\mathcal{N}^{FE} will be large,

such that \mathcal{A}_{μ}^h costly to form and to "invert."

Computational Methodology

- Perspective
- Components and System Synthesis
- Finite Element (FE) Approximation
- Static Condensation Reformulation of FE
- **Model Order Reduction**
- Remarks
- Computational Procedure: PDE App Workflow

In given instantiated component,

$$\nu = \nu(\mu)$$

for local port $i = 1, 2$

for port mode $j = 1, \dots, M$:

$\psi_{i,j}^h = \mathcal{L}_i(\chi_j^{h \text{ fid}} \circ \tau_i^{-1})$ is lifting to

reference domain of port mode j on port i , and

$\varphi_{i,j;\nu}^{h,N} = \psi_{i,j}^h + \eta_{i,j;\nu}^{h,N} \in Z_{i,j}^{h,N \text{ arch}}[\gamma_1, \gamma_2; 0](D_{\bar{\nu}})$ satisfies

$a_{\nu}^{D_{\bar{\nu}}}(\varphi_{i,j;\nu}^h, v) = 0, \forall v \in Z_{i,j}^{h,N}[\gamma_1, \gamma_2; 0](D_{\bar{\nu}})$, subject to

$$\varphi_{i,j;\nu}^h|_{\gamma_{i'}} = \chi_j^h \delta_{ii'}; \quad N \times N$$

where for simplicity all sources reside on ports.

Details

Express $\eta_{i,j;\nu}^{h,N}$ as $1 \leq j \leq M$, $1 \leq i \leq 2$

$$\eta_{i,j;\nu}^{h,N}(\bar{x}) = \sum_{k=1}^N \eta_{i,j,k;\nu}^{h,N} \zeta_{i,j,k}(\bar{x}) \text{ for } \bar{x} \in D_{\bar{\nu}} ;$$

then $\eta_{i,j,k;\nu}^{h,N}$ satisfy

$$\begin{aligned} & \sum_{k=1}^N \left(\int_{D_{\bar{\nu}}} (\kappa(\nabla \zeta_{i,j,k'}^*))^T \mathbb{G}_{\nu} \nabla \zeta_{i,j,k} - k^2 \zeta_{i,j,k}^* \zeta_{i,j,k} \right) |\mathbb{J}_{\nu}| d\bar{x} \eta_{i,j,k;\nu}^{h,N} \\ &= - \int_{D_{\bar{\nu}}} (\kappa(\nabla \zeta_{i,j,k'}^*))^T \mathbb{G}_{\nu} \nabla \psi_{i,j}^h - k^2 \zeta_{i,j,k'}^* \psi_{i,j}^h \Big|_{\mathbb{J}_{\nu}} d\bar{x} \end{aligned}$$

for $1 \leq k' \leq N$.

In given instantiated component,

$$u_{\mu}^{h,M,N} |_{D_{\nu}(\mu)} = \sum_{i=1}^2 \sum_{j=1}^M u_{i,j;\nu}^{h,M,N} (\varphi_{i,j;\nu}^{h,N} \circ \mathcal{T}_{\nu}^{-1})$$

for appropriate coefficients $u_{i,j;\nu}^{h,M,N}$, $1 \leq j \leq M$, $i = 1, 2$.

Form $2M \times 2M$ stiffness matrix $A_{[i,j],[k,\ell];\nu}^{h,M,N}$ (Petrov)-Galerkin :

normal velocity moment on local port i flux
with respect to test port mode j

expressed in terms of

pressure coefficient on local port k
associated with trial port mode ℓ .

We may write stiffness matrix as

$$A_{[i,j],[k,\ell];\nu}^{h,M,N} \equiv \int_{D_{\bar{\nu}}} \left(\kappa(\nabla\psi_{i,j}^{h,*})^T \mathbb{G}_{\nu} \nabla(\psi_{i,j}^h + \eta_{k,\ell;\nu}^{h,N}) - k^2(\psi_{i,j}^{h,*})(\psi_{i,j}^h + \eta_{k,\ell;\nu}^{h,N}) \right) |\mathbb{J}_{\nu}| d\bar{x} ,$$

for $1 \leq i, k \leq 2, 1 \leq j, \ell \leq M$.

...PR-SCRBE-FE

Require on global ports $\Gamma \in G$

continuity of pressure, and

weak continuity of normal velocity

implemented as direct stiffness assembly:

$$\{A_{\nu(\mu)}^{h,M,N}\} \text{ instantiated components} \rightarrow \mathcal{A}_{\mu}^{h,M,N} \quad \mathcal{F}_{\mu}^{h,M,N}$$

where $\mathcal{A}_{\mu}^{h,M,N}$ is $|G|M \times |G|M$ block-sparse.

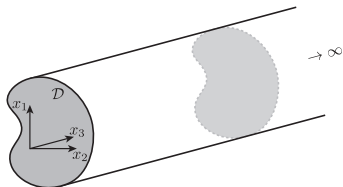
Issues "resolved": $M \ll J^{\text{FE}}$, and

$$N \ll \mathcal{N}^{\text{FE}},$$

such that $\mathcal{A}_{\mu}^{h,M,N}$ is inexpensive to form and to "invert."

Port Reduction, $M \ll J^{\text{FE}}$: Rationale...

Consider a waveguide $\mathcal{D} \times (0, \infty)$,



and find $p(x_1, x_2, x_3)$ such that

$$-\nabla^2 p - k^2 p = 0 \text{ in } \mathcal{D} \times (0, \infty) \quad ,$$

and

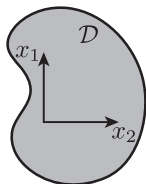
$$p = g \text{ on } (x_1, x_2) \in \mathcal{D}, x_3 = 0,$$

$$\frac{\partial p}{\partial n} = 0 \text{ on } (x_1, x_2) \in \partial \mathcal{D}, 0 < x_3 < \infty,$$

p (say) outgoing bounded wave as $x_3 \rightarrow \infty$.

...Port Reduction, $M \ll J^{\text{FE}}$: Rationale...

Restrict attention to the transverse domain \mathcal{D} ,



and find $(\Upsilon_i(x_1, x_2), \lambda_i)_{i=1, \dots}$ solution of eigenproblem

$$-\nabla_{x_1, x_2}^2 \Upsilon = \lambda \Upsilon, \text{ in } \mathcal{D},$$

$$\frac{\partial \Upsilon}{\partial n} = 0 \text{ on } \partial \mathcal{D};$$

order (real) eigenvalues $\lambda_1 = 0 < \lambda_2 \leq \lambda_3 \leq \dots$

...Port Reduction, $M \ll J^{\text{FE}}$: Rationale — Evanescence

Consider $k \in [\sqrt{\lambda_n}, \sqrt{\lambda_{n+1}})$: then

$\Re\{\cdot e^{i\omega t}\}$

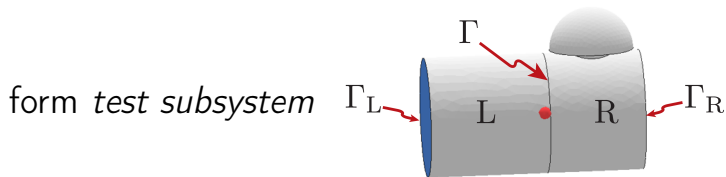
$$p = \sum_{j=1}^n \alpha_j^g \Upsilon_j(x_1, x_2) e^{-i\sqrt{k^2 - \lambda_j} x_3} \\ + \sum_{j=n+1}^{\infty \text{ (or } J^{\text{FE}})} \alpha_j^g \Upsilon_j(x_1, x_2) e^{-\sqrt{\lambda_j - k^2} x_3}$$

for coefficients α_j^g chosen to realize $p(\cdot, \cdot, x_3 = 0) = g$.

For any global port $\Gamma \in G$, higher modes introduced in neighboring components, and at neighboring global ports, will be filtered prior to "arrival" at Γ .

Port Reduction, $M \ll J^{\text{FE}}$: A Library Training Procedure

For all compatible archetype component pairs in Library,



and find $z \in X^h(\text{L}, \text{R})$ such that

$$a_{\nu_L, \nu_R}^{(\text{L}, \text{R})}(z, v) = 0, \quad \forall v \in X^h(\text{L}, \text{R}),$$

for a rich set of Dirichlet conditions on Γ_L , Γ_R , and
admissible parameters ν_L and ν_R .

Collect $z|_{\Gamma} \circ \mathcal{T}_{\nu} \circ \tau$ from all test subsystems in a set S .

Apply POD to S : fiducial port modes $\{\chi_j\}_{j=1, \dots, M}$.

Bubble Reduction, $N \ll \mathcal{N}^{\text{FE}}$: Rationale

For any archetype component in Library,

for local port $i = 1, 2$,

for port mode $j = 1, \dots, M$,

$$\eta_{i,j;\nu}^h \in \underbrace{\{\eta_{i,j;\nu}^h \text{ on } D_{\bar{\nu}} \mid \nu \in \mathcal{V}\}}_{\text{low-dimensional smooth manifold}} \subset \underbrace{X_{[\gamma_1, \gamma_2; 0]}^h(D_{\bar{\nu}})}_{\text{high-dimensional space}} ;$$

note that

$$\nu_{\text{local}} \in \mathcal{V} \subset \mathbb{R}^V, \mu_{\text{model}} \in \mathcal{P} \subset \mathbb{R}^P$$

for (typically) $V \ll P$ — *components divide and conquer.*

Bubble Reduction, $N \ll \mathcal{N}^{\text{FE}}$: A Library Training Procedure

For each archetype component in Library,

for local port $i = 1, 2$,

for port mode $j = 1, \dots, M$,

form $Z_{i,j}^{h,N}[\gamma_1, \gamma_2:0]$ as RB Lagrangian snapshot space \perp -ized

$$Z_{i,j}^{h,N}[\gamma_1, \gamma_2:0] \equiv \text{span}\{\eta_{i,j}^h; \nu_{i,j}^n, 1 \leq n \leq N_{i,j}\}$$

for quasi-optimal parameter values

$$\{\nu_{i,j}^1 \in \mathcal{V}, \dots, \nu_{i,j}^N \in \mathcal{V}\}$$

selected by the RB Weak-Greedy procedure.

Computational Methodology

- Perspective
- Components and System Synthesis
- Finite Element (FE) Approximation
- Static Condensation Reformulation of FE
- Model Order Reduction
- **Remarks**
- Computational Procedure: PDE App Workflow

Under certain hypotheses, the best fits associated with
the port reduced spaces, $\text{span}\{\chi_j, 1 \leq j \leq M\}$,
and
the bubble reduced spaces, $Z_{i,j}^{h,N}$,
converge at rates similar to the corresponding
Kolmogorov M (respectively, N) width.
The (Petrov-)Galerkin projections are optimal to within
a (Model, μ and M, N)-dependent stability constant.

Verification (and Validation)

A *posteriori* error **indicators** play a role in

optimal choice of snapshots $\rightarrow Z_{i,j}^{h,N}$

and

optimal choice of M and N .

Each Model is verified over $\Xi_{\text{verification}} \subset \mathcal{P}$:

refinement in $h \downarrow$, $M \uparrow$, and $N \uparrow$;

reference to appropriate closed-form approximations;

comparison to 3rd-party computations and experiments.

Verification of each Model improves

archetype components: convergence of *Library*.

Computational Methodology

- Perspective
- Components and System Synthesis
- Finite Element (FE) Approximation
- Static Condensation Reformulation of FE
- Model Order Reduction
- Remarks
- Computational Procedure: PDE App Workflow

Prepare Online Dataset \mathbb{D} for Library:

archetype component reference FE meshes;

archetype *affine* component mappings \mathcal{T}_ν ;

port modes $\chi_j^h, 1 \leq j \leq M$ (for each port type);

RB spaces $Z_{i,j}^{h,N}$ for each archetype component,
local port i , and port mode j ;

(Petrov-)Galerkin parameter-independent inner products.

Role of components:

no Models formed or evaluated in Offline I stage;

all Models in Online stage amortize Offline I effort.

A typical term in

$$A_{[i,j],[k,l];\nu}^{h,M,N} \equiv \int_{D_{\bar{\nu}}} (\kappa(\nabla\psi_{i,j}^{h*})^T \mathbb{G}_{\nu} |\mathbb{J}_{\nu}| \nabla(\psi_{i,j}^h + \eta_{k,l;\nu}^{h,N})) + \dots$$

leads to inner product

$$\sum_{n=1}^N \eta_{k,\ell,n;\nu}^{h,N} \int_{D_{\bar{\nu}}} (\kappa(\nabla\psi_{i,j}^{h*})_1 \underbrace{(\mathbb{G}_{\nu})_1 |\mathbb{J}_{\nu}|}_{\text{EIM expansion}} (\nabla(\psi_{i,j}^h + \zeta_{k,\ell,n}))_1) \cdot$$

Online: \mathbb{D} ; Model; $\mu \in \mathcal{P} \rightarrow u_{\mu}^{h,M,N}, s_{\mu}^{h,M,N}$

Fast

Web-User-Interface (WUI) Cloud Implementation

Query the PDE App:

input $\mu \in \mathcal{P}$,

User

synthesize Model from (say) script,

Model Server

invoke Online Dataset \mathbb{D}

Compute Server

form and solve Schur complement,

Compute Server

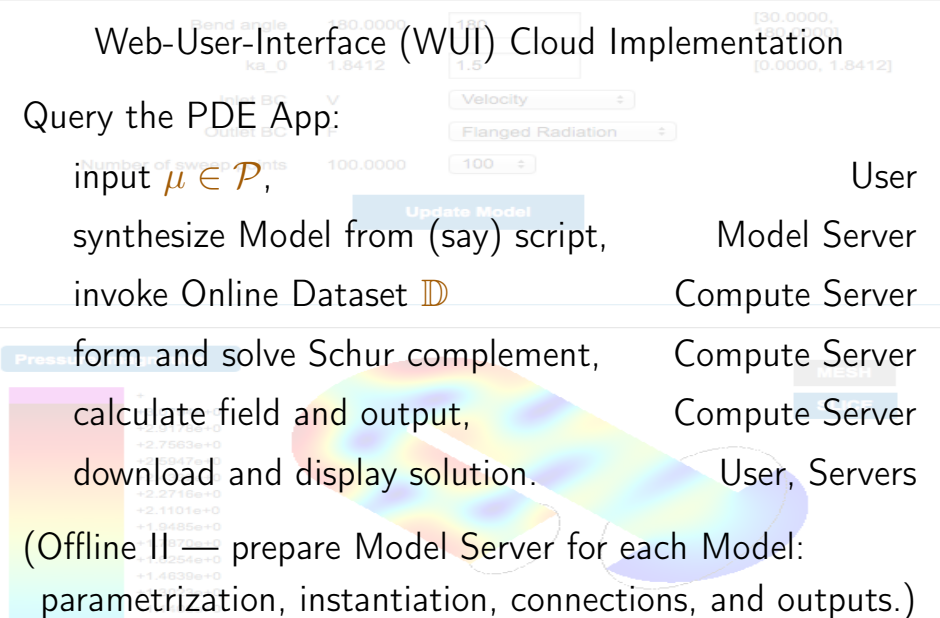
calculate field and output,

Compute Server

download and display solution.

User, Servers

(Offline II — prepare Model Server for each Model: parametrization, instantiation, connections, and outputs.)



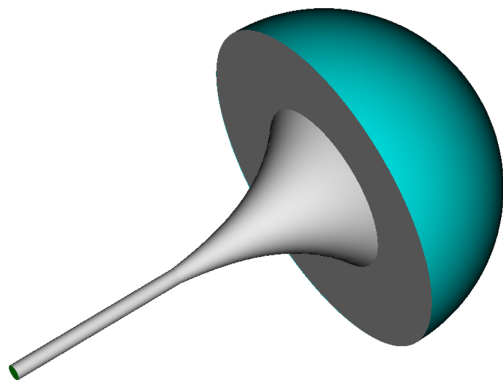
Acoustics Ducts: PDE App Examples

- A Flanged Exponential Horn
- An Expansion Chamber
- A Circular Duct with Toroidal Bend
- An Extended-Tube Expansion Chamber (ETEC)

Acoustics Ducts: PDE App Examples

- A Flanged Exponential Horn
- An Expansion Chamber
- A Circular Duct with Toroidal Bend
- An Extended-Tube Expansion Chamber (ETEC)

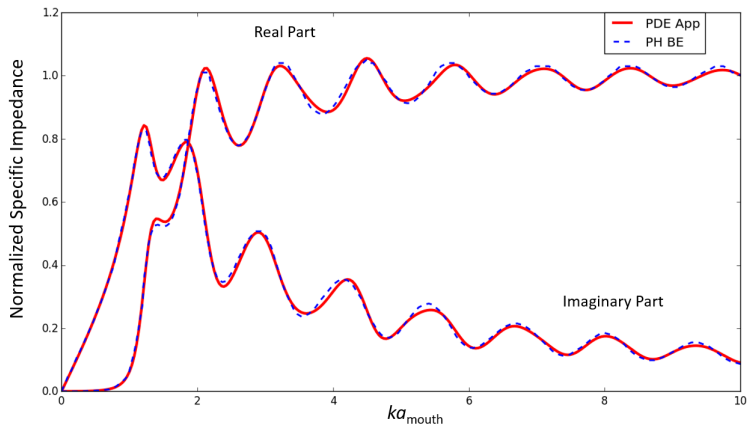
Model: Parametrization and Spatial Domain



$$\mu \equiv (L/a_0, m^{\text{horn}}, a_{\text{mouth}}/a_0, ka_0)$$
$$\in \mathcal{P} \equiv [2, 20] \times [0.0334, 0.1666] \times [4, 12] \times [0, 1]$$

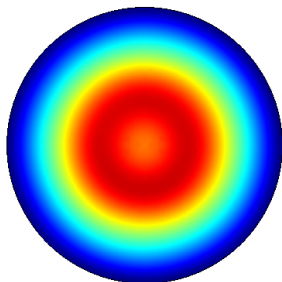
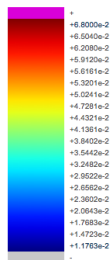
Throat Impedance

Parameters: $m^{\text{horn}} = 0.1076$, $a_{\text{mouth}}/a_0 = 10.67$.

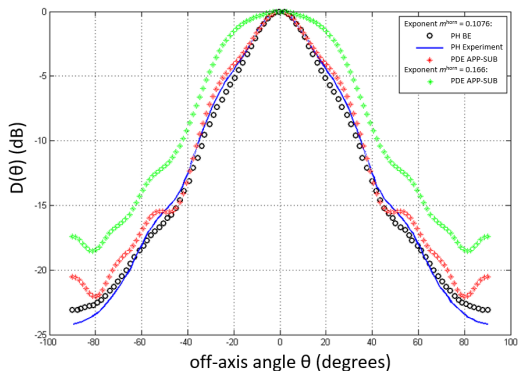


PH: Post & Hixson, PhD Thesis, 1974.

Pressure, magnitude



Nearfield



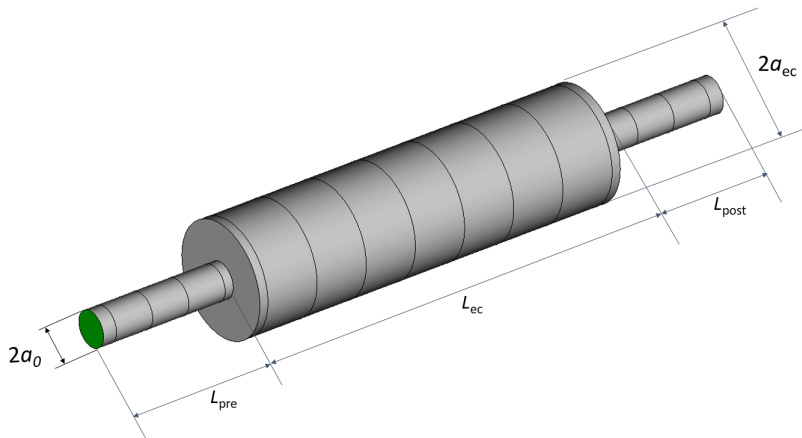
Farfield

Modulus of Pressure

Acoustics Ducts: PDE App Examples

- A Flanged Exponential Horn
- An Expansion Chamber
- A Circular Duct with Toroidal Bend
- An Extended-Tube Expansion Chamber (ETEC)

Model: Parametrization and Spatial Domain

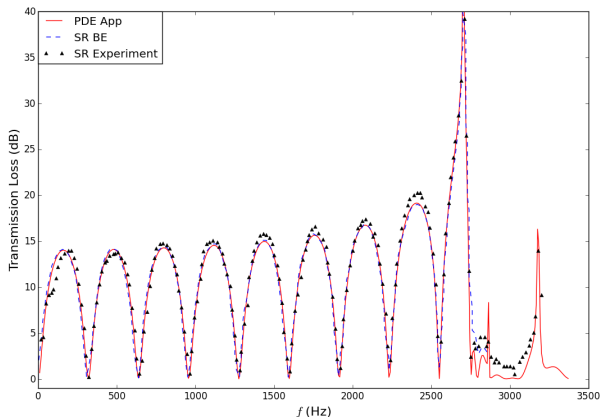


$$\mu \equiv (L_{pre}/a_0, L_{post}/a_0, L_{ec}/a_0, a_{ec}/a_0, ka_0)$$
$$\in \mathcal{P} \equiv [4, 12]^2 \times [1.5, 25] \times [1.5, 6.5] \times [0, 1.5]$$

Transmission Loss

Parameters: $L_{ec}/a_0 = 22.26$, $a_{ec}/a_0 = 3.152$;

$a_0 = 0.0243$ cm.

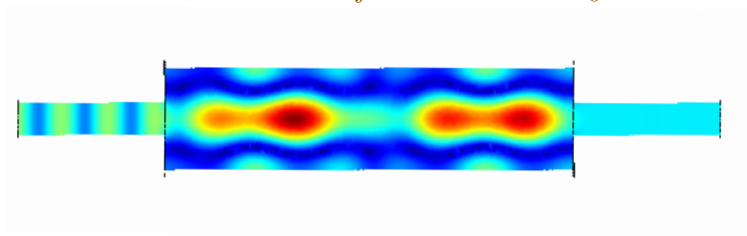


SR: Selamat and Radavich, J Sound Vibration, 1997.

Visualization: Excitation of (Axisymmetric) Higher Modes

Parameters: $L_{ec}/a_0 = 22.26$, $a_{ec}/a_0 = 3.1525$;

$f = 2.8$ kHz, $a_0 = 0.0243$ cm.

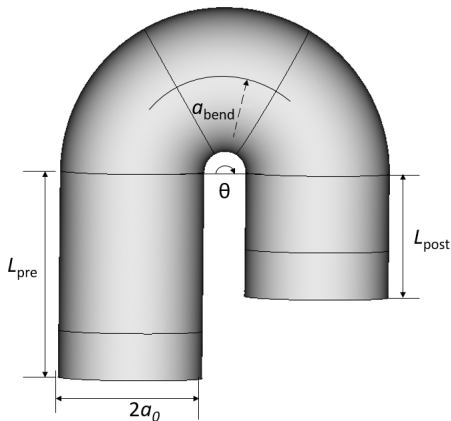
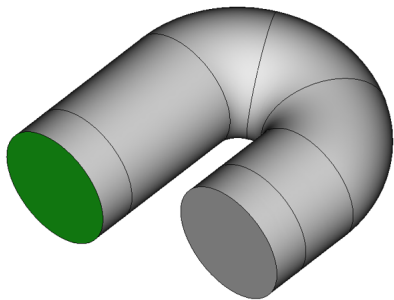


Modulus of Pressure

Acoustics Ducts: PDE App Examples

- A Flanged Exponential Horn
- An Expansion Chamber
- A Circular Duct with Toroidal Bend
- An Extended-Tube Expansion Chamber (ETEC)

Model: Parametrization and Spatial Domain



$$\mu \equiv (L_{pre}/a_0, L_{post}/a_0, a_{bend}/a_0, \theta_{bend}, ka_0)$$
$$\in \mathcal{P} \equiv [1.5, 15]^2 \times [1.2, 3] \times [30^\circ, 180^\circ] \times [0, 1.8412]$$

PDE Apps for Education The PDE App Project Team

Quick Start

- ☑ List of Models
 - ☑ Acoustic Ducts
 - Circular Duct with Bend
 - Expansion Chamber
 - ETEC Muffler
 - ☑ Acoustic Ducts **SUB**

The PDE App Project Team

Principal Investigators

DBP Huynh (Akselos S.A.) and AT Patera* (MIT)

Academic Contributors

P Dahl (U Washington)

SC Joyce (SUTD)

D Vignon (MIT)

M Yano (U Toronto)

None of the academic contributors has any financial interest in Akselos, S.A.

Akselos Contributors

D Knezevic, B Sabbey (Akselos, Boston)

T Hoang, L Nguyen, T Nguyen (Akselos, Ho Chi Minh City)

T Leurent, S Vallaghé (Akselos, Lausanne)

Sponsors

The PDE App methodology, software, server, and website is, or has been, funded by the AFOSR/OSD, the ONR, the Deshpande Center at MIT, SUTD and the SUTD-MIT International Design Center, a Ford Professorship of Engineering at MIT, the MIT Department of Mechanical Engineering, and Akselos, S.A.

**Akselos S.A. licenses technology developed in the MIT research group of AT Patera. AT Patera has no financial interest in Akselos S.A.*

WUI: Parameter Specification

ACOUSTIC DUCTS - CIRCULAR DUCT WITH TOROIDAL BEND

SOLVE

MODEL INFO

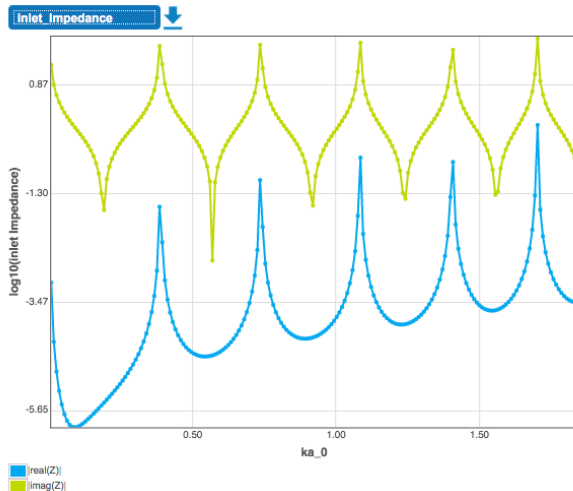
HOW TO USE

LOGS

	Current value	New value	Range
L_pre/a_0	2.8571	<input type="text" value="2.8571"/>	[1.5000, 15.0000]
L_post/a_0	1.7143	<input type="text" value="1.7143"/>	[1.5000, 15.0000]
a_bend/a_0	1.2857	<input type="text" value="1.2857"/>	[1.2000, 3.0000]
Bend angle	180.0000	<input type="text" value="180"/>	[30.0000, 180.0000]
ka_0	1.8200	<input type="text" value="1.82"/>	[0.0000, 1.8412]
Inlet BC	V	<input type="text" value="Velocity"/>	
Outlet BC	V	<input type="text" value="Velocity"/>	
Number of sweep points	200.0000	<input type="text" value="200"/>	

Update Model

WUI: Output

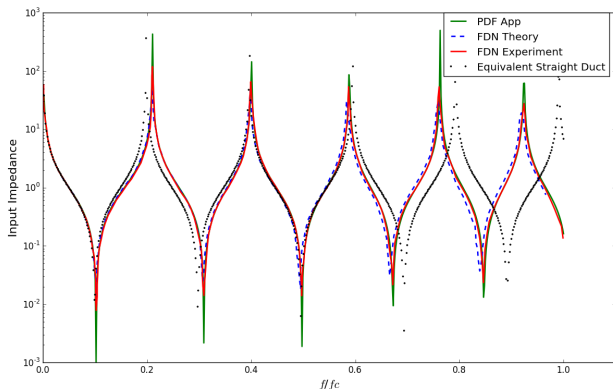


Response Time (all-inclusive) 8.4 seconds:
4-core GCE instance and commodity Internet.

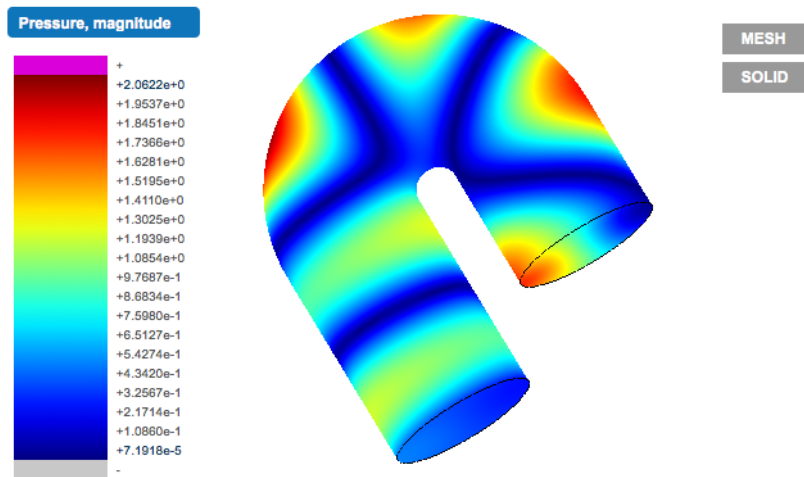
Inlet Impedance (Reactive)

Parameters: $L_{\text{pre}}/a_0 = 2.8571$, $L_{\text{post}}/a_0 = 1.7143$,
 $a_{\text{bend}}/a_0 = 1.2857$, $\theta_{\text{bend}} = 180^\circ$.

Boundary Conditions: velocity-velocity.



FDN: Félix, Dalmont, and Nederveen, JASA, 2012.

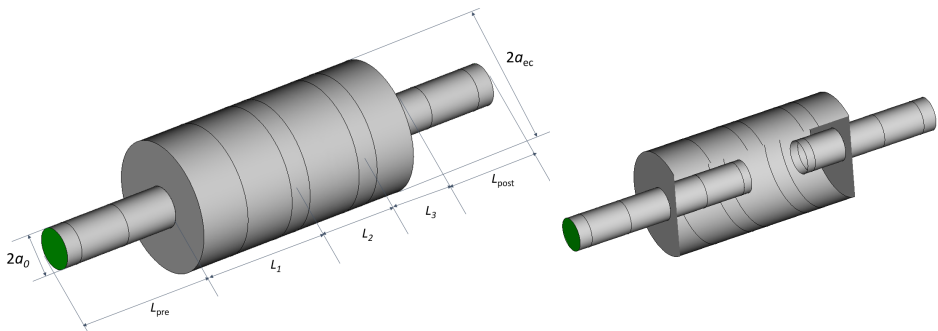


Response Time (all-inclusive) 8.4 seconds:
4-core GCE instance and commodity Internet.

Acoustics Ducts: PDE App Examples

- A Flanged Exponential Horn
- An Expansion Chamber
- A Circular Duct with Toroidal Bend
- An Extended-Tube Expansion Chamber (ETEC)

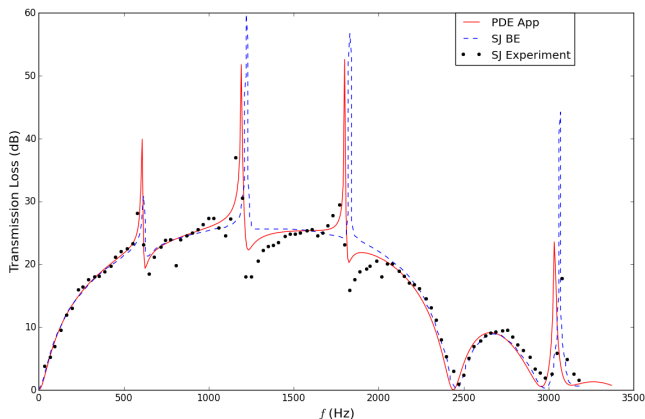
Model: Parametrization and Spatial Domain



$$\mu \equiv (L_{\text{pre}}/a_0, L_{\text{post}}/a_0, L_1/a_0, L_2/a_0, L_3/a_0, a_{\text{ec}}/a_0, ka_0) \\ \in \mathcal{P} \equiv [2, 6]^2 \times [2, 16]^3 \times [1.5, 4.0] \times [0, 1.5]$$

Transmission Loss

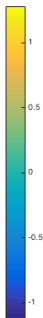
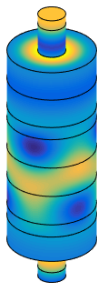
Parameters: $L_1/a_0 = 5.391$, $L_2/a_0 = 3.716$,
 $L_3/a_0 = 2.510$, $a_{ec}/a_0 = 3.152$; $a_0 = 0.0243$ cm.



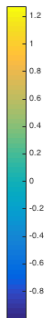
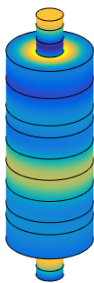
SJ: Selamet and Ji, J Sound Vibration, 1999.

Achtung!

Pressure, real part



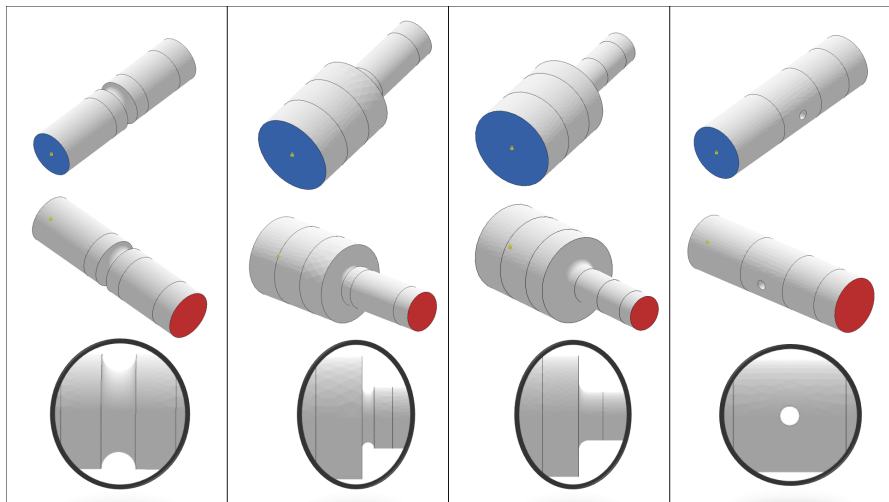
Pressure, real part



Issues: physical stability, numerical stability, . . .
. . . components, training, projection.

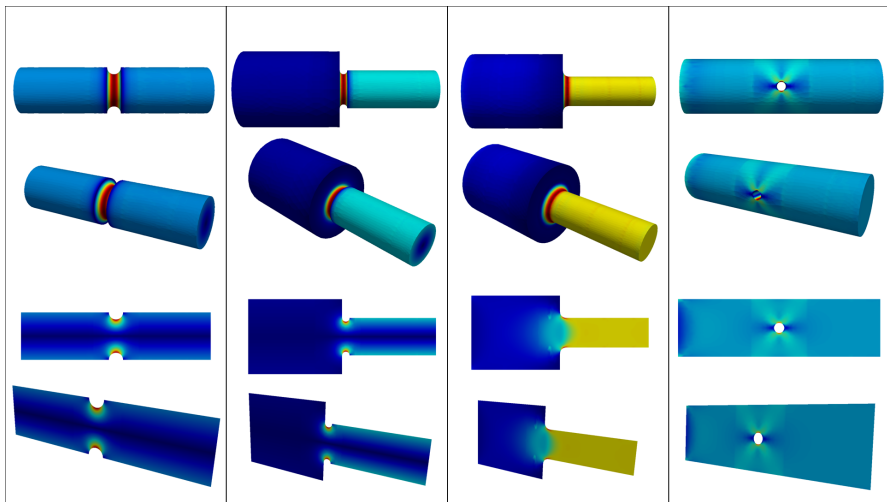
Elastic Shafts: PDE App Examples — briefly

A Family \mathcal{F} of Models



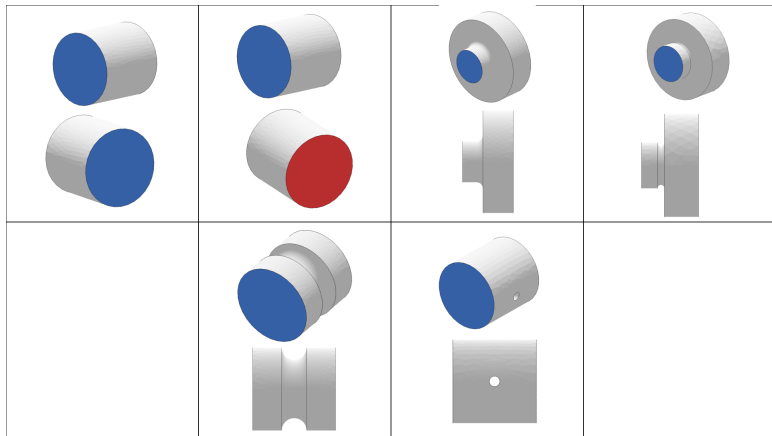
\mathcal{F} : Elasticity, Shafts; Stress Concentration Factors (SCFs)

A Family of Models, \mathcal{F}



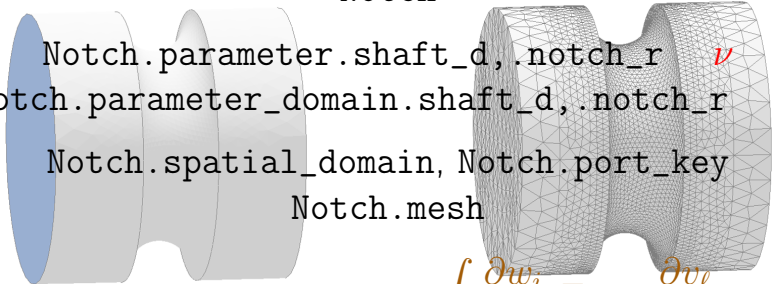
\mathcal{F} : Elasticity, Shafts; SCFs

A Library \mathcal{L} of Archetype Components for \mathcal{F} Port Key



A Parametrized Archetype Component in \mathcal{L}

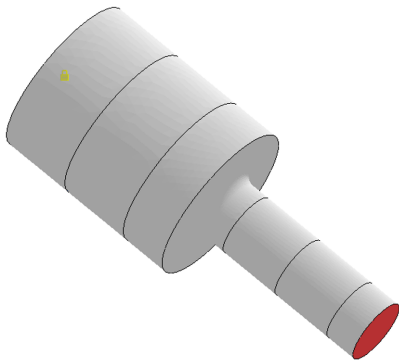
Notch



`Notch.parameter.shaft_d, .notch_r` ✓
`Notch.parameter_domain.shaft_d, .notch_r` ✓
`Notch.spatial_domain, Notch.port_key`
`Notch.mesh`

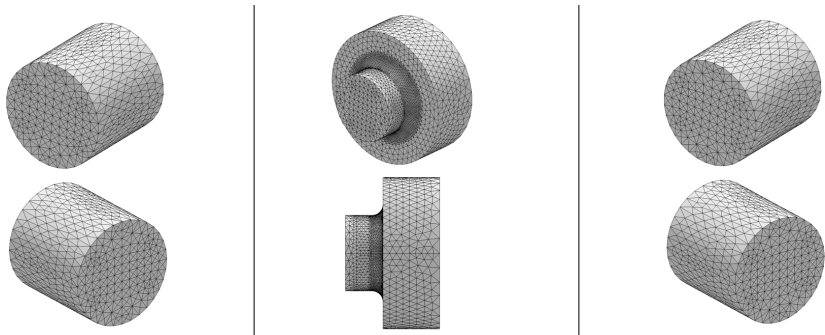
$$\text{Notch.PDE.forms.a} = \int \frac{\partial w_i}{\partial x_j} E_{ijklm} \frac{\partial v_\ell}{\partial x_m}$$
$$\text{Notch.PDE.forms.f} = 0$$

Synthesis: Model_Shoulder_Fillet in \mathcal{F}



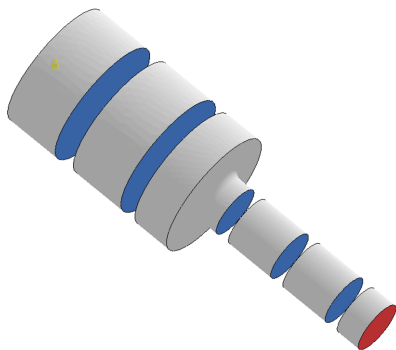
Model_Shoulder_Fillet
 $\mu \equiv (L, D_1/D_2, r_{\text{fillet}}/D_2, E)$

Synthesis: Model_Shoulder_Fillet in \mathcal{F}



(Relevant) Parametrized Archetype Components:
Tension_Torsion_Load,
Shoulder_Fillet, Circular_Shaft

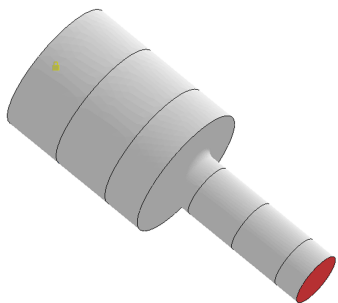
Synthesis: Model_Shoulder_Fillet in \mathcal{F}



$$\mu \equiv (L, D_1/D_2, r_{\text{fillet}}/D_2, E)$$

→ (ν) Parameter-Instantiated (Archetype) Components

Synthesis: Model_Shoulder_Fillet in \mathcal{F}



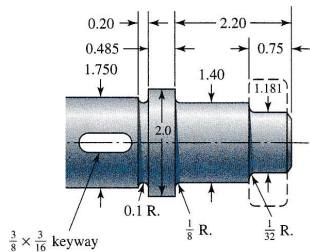
Geometry



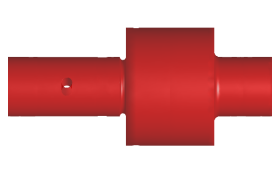
Mesh

Connection of Local Ports (μ) \rightarrow
Global Ports and Assembled *System*

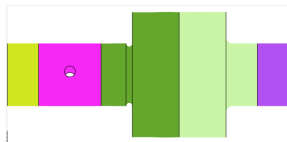
Synthesis: Model_Shaft in $\mathcal{F}_{\mathcal{L}}$ — Formulation



Shigley *et al.* Problem 18-81

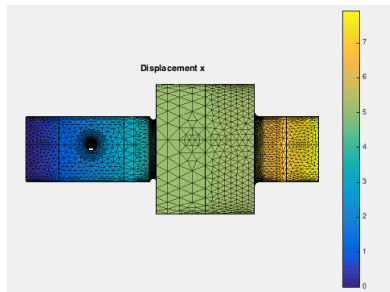


Model: $\mu \in \mathcal{P} \rightarrow \Omega_{\mu}$

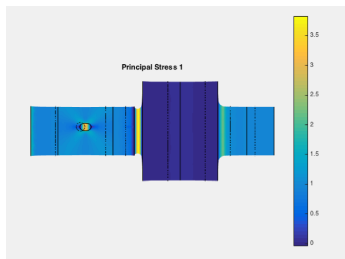


Assembled System $\leftarrow \mathcal{L}$

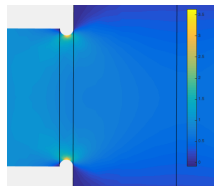
Synthesis: Model_Shaft in \mathcal{F}_L — Solution (accuracy?)



Axial Displacement



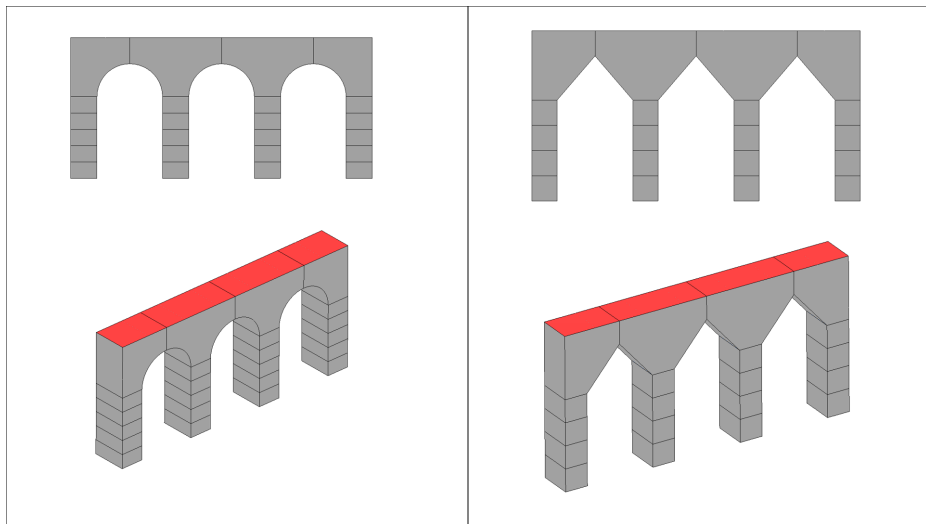
Principal Stress: σ_1



Axial Stress: σ_{11}

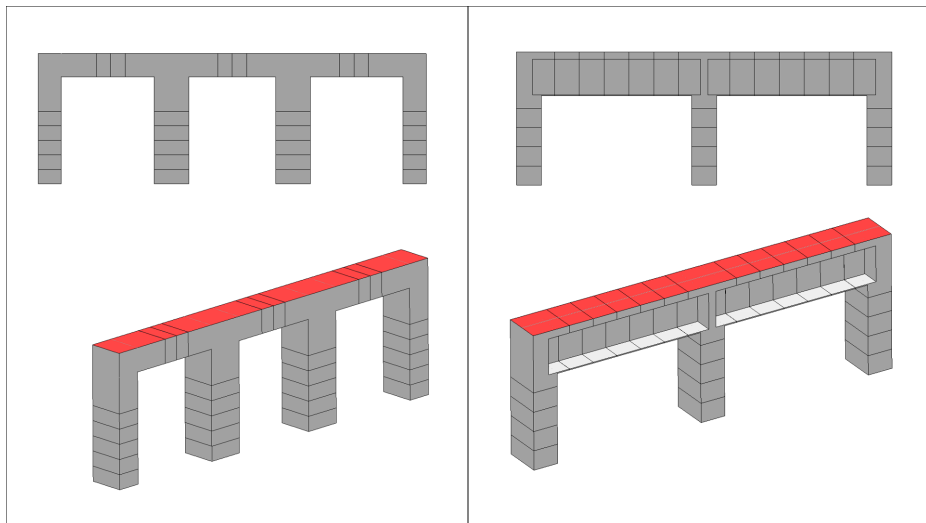
Lintels and Arches: PDE App Examples — briefly

A Family \mathcal{F} : Models...



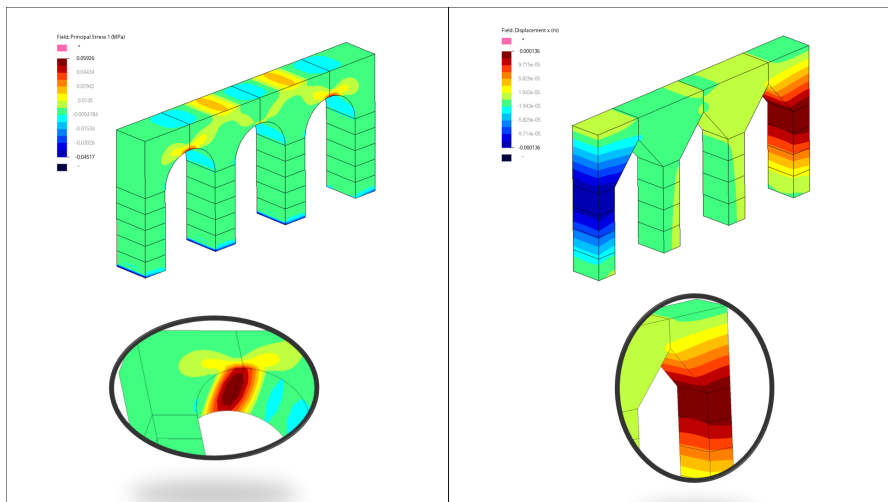
\mathcal{F} : Elasticity, Lintels and Colonnades; Max $|u|$, Max σ_1

A Family \mathcal{F} : Models...



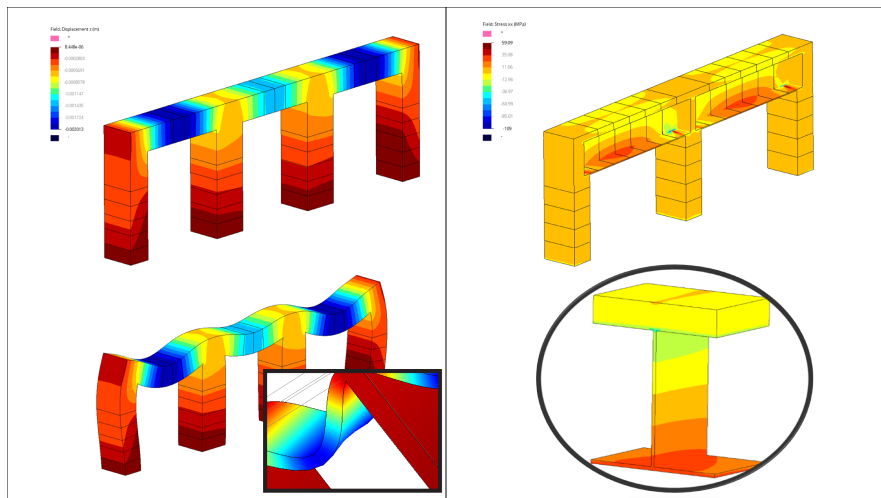
\mathcal{F} : Elasticity, Lintels and Colonnades; Max $|u|$, Max σ_1

A Family \mathcal{F} : ... and Representative Solutions



\mathcal{F} : Elasticity, Lintels and Colonnades; Max $|u|$, Max σ_1

A Family \mathcal{F} : ... and Representative Solutions



\mathcal{F} : Elasticity, Lintels and Colonnades; Max $|u|$, Max σ_1

A Parametrized Archetype Component

I-beam

I-beam.spatial_domain, I-beam.mesh

I-beam.ports

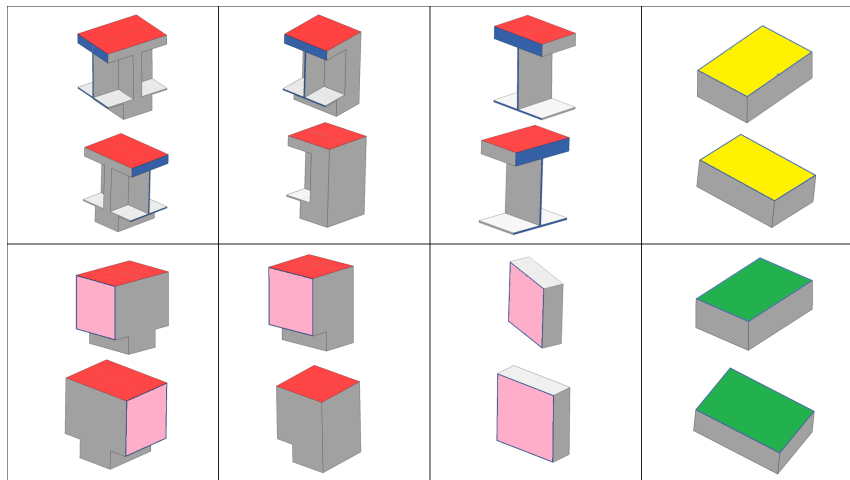
I-beam.parameter.web_H, .flange_t ν

I-beam.parameter_domain.web_H, .flange_t ν

$$\text{I-beam.PDE.forms.a} = \int \frac{\partial w_i}{\partial x_j} E_{ijklm} \frac{\partial v_l}{\partial x_m}$$

$$\text{I-beam.PDE.forms.f} = - \int_{B_{\text{load}}} \delta_{i3}$$

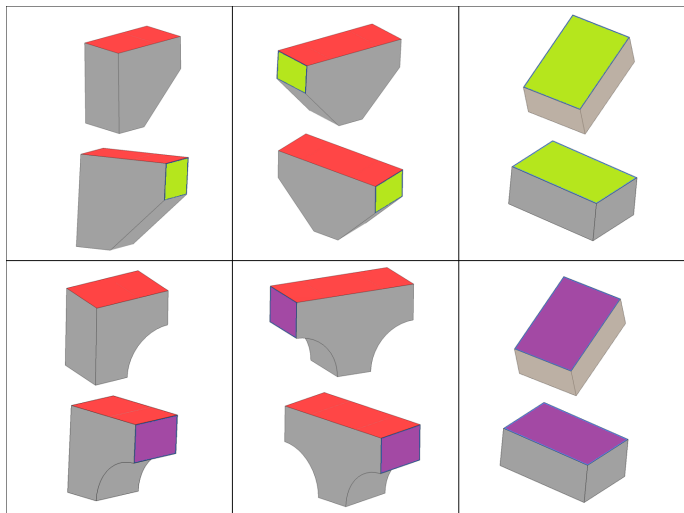
A Library \mathcal{L} of Parametrized Archetype Components for \mathcal{F}



Admissible connections:

ports of common color \leftarrow common port key.

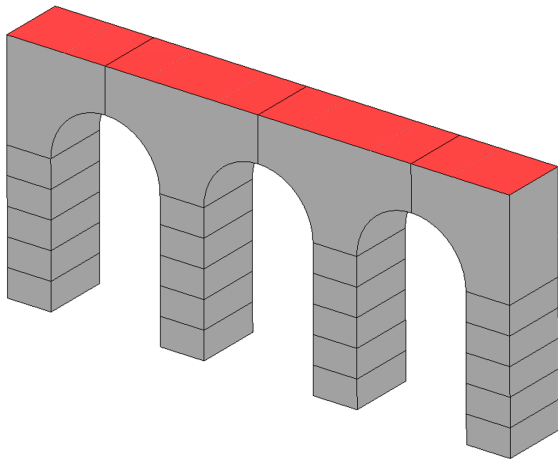
A Library \mathcal{L} of Parametrized Archetype Components for \mathcal{F}



Admissible connections:

ports of common color \leftarrow common port key.

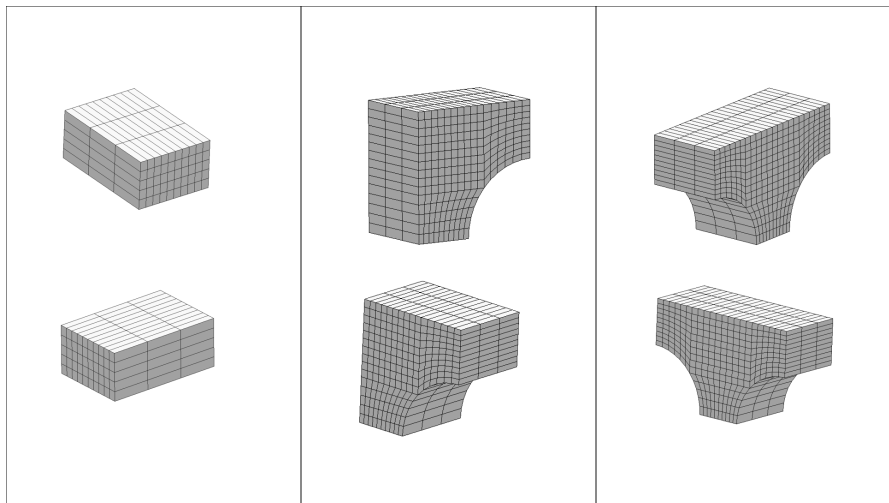
Synthesis: Model_Roman_Arch in \mathcal{F}



Model_Roman_Arch

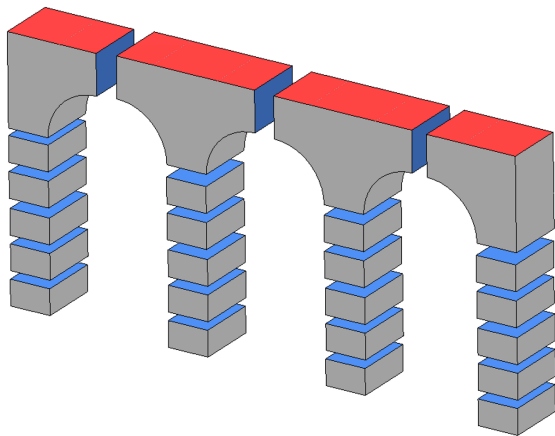
$$\mu \equiv (H_{\text{col}}/D, W_{\text{col}}/D, r_{\text{arch}}/D, n_{\text{arches}}, E) \in \mathcal{P}$$

Synthesis: Model_Roman_Arch in \mathcal{F}



(Relevant) Parametrized Archetype Components:
Column, Arch_End, Arch_Middle

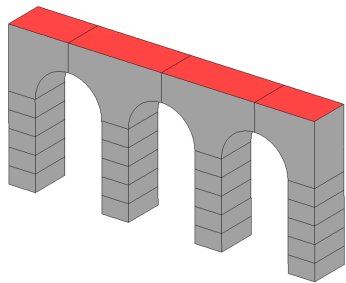
Synthesis: Model_Roman_Arch in \mathcal{F}



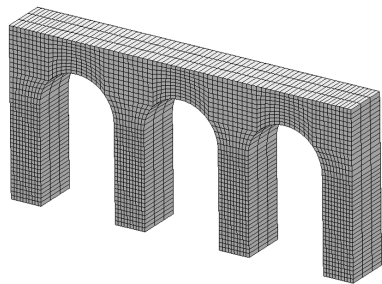
$$\mu \equiv (H_{\text{col}}/D, W_{\text{col}}/D, r_{\text{arch}}/D, n_{\text{arches}}, E) \in \mathcal{P}$$

→ ν Parameter-Instantiated (Archetype) Components

Synthesis: Model_Roman_Arch in \mathcal{F}



Geometry



Mesh

Connection of Local Ports (μ) \rightarrow
Global Ports and Assembled *System*

References

A Few References. . .

BO Almroth, P Stern, and FA Brogan. Automatic choice of global shape functions in structural analysis. *AIAA J*, 1978.

I Babuska and R Lipton. Optimal local approximation spaces for generalized finite element methods with application to multiscale problems. *Multiscale Modeling and Simulation*, 9:373–406, 2011.

M Barrault, Y Maday, N. Nguyen, and A Patera, An empirical interpolation method: Application to efficient reduced-basis discretization of partial differential equations. *CR Acad Sci Paris, Série I* 339:667–672, 2004.

P Binev, A Cohen, W Dahmen, R DeVore, G Petrova, and P Wojtaszczyk. Convergence rates for greedy algorithms in reduced basis methods. *SIAM J Math Anal*, 43(3):1457–1472, 2011.

F Bourquin. Component mode synthesis and eigenvalues of second order operators: discretization and algorithm. *M2AN*, 26(3):385–423,1992.

R Craig and M Bampton. Coupling of substructures for dynamic analyses. *AIAA J*, 1968.

JL Eftang and AT Patera. A port-reduced static condensation reduced basis element method for large component-synthesized structures: Approximation and a posteriori error estimation. *Advanced Modeling and Simulation in Engineering Sciences*, 1:3, 2013.

... A Few References...

JL Eftang and AT Patera. Port reduction in component-based static condensation for parametrized problems: Approximation and a posteriori error estimation. *IJNME*, 96(5):269–302, 2013.

S Félix, J-P Dalmont, and CJ Nederveen. Effects of bending portions of the air column on the acoustical resonances of a wind instrument. *JASA*, 131 (5):4164–4172, 2012.

B Haasdonk and M Ohlberger. Reduced basis method for finite volume approximations of parametrized linear evolution equations. *M2AN*, 42(2):277–302, 2008.

JS Hesthaven, G Rozza, and B Stamm. Certified Reduced Basis Methods for Parametrized Partial Differential Equations. Series: Springer Briefs in Mathematics, Edition Number 1, Springer International Publishing, 2016.

U Hetmaniuk and R Lehoucq. A special finite element method based on component mode synthesis. *M2AN*, 44(3):401–420, 2010.

DBP Huynh, DJ Knezevic, and AT Patera. A Laplace transform certified reduced basis method; Application to the heat equation and wave equation. *CR Acad Sci Paris Series I*, 349(7-8):401–405, 2011.

DBP Huynh, DJ Knezevic, JW Peterson, and AT Patera. High-fidelity real-time simulation on deployed platforms. *Computers and Fluids*, 43(1):74–81, 2011.

... A Few References ...

DBP Huynh, DJ Knezevic, and AT Patera. A static condensation reduced basis element method: Approximation and a posteriori error estimation. *M2AN*, 47(1): 213–251, 2013.

DBP Huynh, DJ Knezevic, and AT Patera. A static condensation reduced basis element method: Complex problems. *CMAME*, 259:197–216, 2013.

WC Hurty. On the dynamics of structural systems using component modes. *AIAA paper no 64-487*, 1964.

H Jakobsson, F Bengzon, and M Larson. Adaptive component mode synthesis in linear elasticity. *IJNME*, 86(7):829–844, 2011.

Y Maday and EM Rønquist. The reduced basis element method: Application to a thermal fin problem. *SIAM JSC*, 26(1):240–258, 2004.

ML Munjal, *Acoustics of Ducts and Mufflers*, Second Edition, Wiley, 2014.

AK Noor and JM Peters. Reduced basis technique for nonlinear analysis of structures. *AIAA J*, 1980.

JT Post and EL Hixson. A modeling and measurement study of acoustic horns. PhD Thesis, University of Texas at Austin, 1994.

... A Few References ...

TA Porsching. Estimation of the error in the reduced basis method solution of nonlinear equations. *Math Comp*, 45:487–496, 1985.

A Quarteroni, A Manzoni, and F Negri. *Reduced Basis Methods for Partial Differential Equations. An Introduction*. Series: La Matematica per il 3+2, Volume 92, Springer International Publishing, 2016.

WC Rheinboldt. On the theory and error estimation of the reduced basis method for multi-parameter problems. *Nonlinear Anal*, 21:849–858, 1993.

G Rozza, DBP Huynh, and AT Patera. Reduced basis approximation and a posteriori error estimation for affinely parametrized elliptic coercive partial differential equations. *Arch Comput Methods Eng*, 15(3):229–275, 2008.

A Selamet and ZL Ji. Acoustic attenuation performance of circular expansion chambers with extended inlet/outlet. *Journal of Sound and Vibration*, 223, 197-212, 1999.

A Selamet and PM Radavich. The effect of length on the acoustic attenuation performance of concentric expansion chambers: An analytical, computational and experimental investigation. *Journal of Sound and Vibration*, 201(4):407–426, 1997.

K Smetana and AT Patera. Optimal local approximation spaces for component-based static condensation procedures. *SIAM JSC* (submitted February 2015).

... A Few References

S Vallaghé, DBP Huynh, D Knezevic, TL Nguyen, and AT Patera. Component-based reduced basis for parametrized symmetric eigenproblems. *Advanced modeling and simulation in engineering sciences*, 2:7, 2015.

K Veroy, C Prud'homme, DV Rovas, and AT Patera. *A posteriori* error bounds for reduced-basis approximation of parametrized noncoercive and nonlinear elliptic partial differential equations. AIAA Paper No. 2003-3847: 1-18, 2003.

EL Wilson. The static condensation algorithm. *Int J Num Methods Engr*, 8(1):198-203, 1974.

K Wong. The “Appification” of Simulation. *Desktop Engineering*, April 1, 2015.